Molecular Cell
Article

Structural and Functional Analysis of the *E. coli* NusB-S10 Transcription Antitermination Complex

Xiao Luo,[1] He-Hsuan Hsiao,[2] Mikhail Bubunenko,[3,4] Gert Weber,[1] Donald L. Court,[3] Max E. Gottesman,[5,*] Henning Urlaub,[2] and Markus C. Wahl[1,6,*]
[1]Research Group X-Ray Crystallography
[2]Research Group Bioanalytical Mass Spectrometry, Am Faßberg 11
Max-Planck-Institute for Biophysical Chemistry, D-37077 Göttingen, Germany
[3]Gene Regulation and Chromosomal Biology Laboratory, Center for Cancer Research
[4]Basic Research Program, SAIC-Frederick, Inc.
National Cancer Institute at Frederick, Frederick, MD 21702, USA
[5]Departments of Microbiology and Biochemistry and Molecular Biophysics, Columbia University Medical Center, New York, NY 10032, USA
[6]Department of Medicine, Georg-August-University Göttingen, Justus-von-Liebig-Weg 11, D-37077 Göttingen, Germany
*Correspondence: meg8@columbia.edu (M.E.G.), mwahl@gwdg.de (M.C.W.)
DOI 10.1016/j.molcel.2008.10.028

SUMMARY

Protein S10 is a component of the 30S ribosomal subunit and participates together with NusB protein in processive transcription antitermination. The molecular mechanisms by which S10 can act as a translation or a transcription factor are not understood. We used complementation assays and recombineering to delineate regions of S10 dispensable for antitermination, and determined the crystal structure of a transcriptionally active NusB-S10 complex. In this complex, S10 adopts the same fold as in the 30S subunit and is blocked from simultaneous association with the ribosome. Mass spectrometric mapping of UV-induced crosslinks revealed that the NusB-S10 complex presents an intermolecular, composite, and contiguous binding surface for RNAs containing BoxA antitermination signals. Furthermore, S10 overproduction complemented a *nusB* null phenotype. These data demonstrate that S10 and NusB together form a BoxA-binding module, that NusB facilitates entry of S10 into the transcription machinery, and that S10 represents a central hub in processive antitermination.

INTRODUCTION

As one strategy to increase the functional diversity of their proteomes, organisms make use of "moonlighting" proteins that can function in more than one cellular context (Jeffery, 1999). In many cases, the molecular basis for the dual activity of a particular protein is unknown. Prime among such multipurpose proteins are the ribosomal (r-) proteins, many of which exhibit additional extraribosomal functions (Wool, 1996). For example, transcription and translation are directly coupled in prokaryotes, and a number of r-proteins moonlight as transcription factors (Squires and Zaporojets, 2000). As the first such example, bacterial S10 was initially defined as an r-protein before an additional role in transcription was discovered (Friedman et al., 1981).

During lytic growth, phage λ switches from early to delayed early gene expression by processive transcription antitermination, which relies on the phage-encoded protein N, an RNA control sequence (N-utilization site, Nut; comprising two linear elements, BoxA and a "spacer," followed by a stem loop, BoxB) and four host N-utilization substances (NusA, NusB, NusE, and NusG) (Friedman and Court, 1995; Friedman and Gottesman, 1983). NusE is identical to r-protein S10 (Friedman et al., 1981). N, Nut RNA, and the Nus factors form a ribonucleoprotein complex on the surface of RNA polymerase (RNAP), in which RNA and protein factors engage in numerous, predominantly weak and cooperative contacts (Mogridge et al., 1995). The N-Nut-Nus factor complex accompanies RNAP during elongation via RNA looping (Whalen and Das, 1990) and promotes progressive transcription elongation through downstream intrinsic and factor-dependent termination sites (Weisberg and Gottesman, 1999). *Escherichia coli* and other bacteria utilize a similar mode of processive antitermination during rRNA gene (*rrn*) transcription (Li et al., 1984; Quan et al., 2005). Other r-proteins, including S4, additionally participate in this latter process (Torres et al., 2001). In contrast, prophage HK022, to avoid superinfection by λ, expresses the Nun protein, a transcription factor related to N, which competes with N at λ Nut sites and, after enlisting the four Nus factors, provokes transcription termination on the λ chromosome (Robert et al., 1987).

S10 is an important architectural element in the 30S ribosomal subunit, as revealed by reconstitution (Mizushima and Nomura, 1970) and crystal structure analyses (Schluenzen et al., 2000; Wimberly et al., 2000). During antitermination, S10 forms a stable complex with NusB (Mason et al., 1992) that has enhanced affinity for BoxA-containing RNAs compared to NusB alone (Lüttgen et al., 2002; Mogridge et al., 1998; Nodwell and Greenblatt, 1993). Since BoxA is strictly conserved in all seven *rrn* operons of *E. coli*, whereas the BoxB-like element is dispensable for *rrn* antitermination (Berg et al., 1989), association of NusB, S10, and BoxA is considered as a key nucleation event during processive antitermination (Greive et al., 2005).

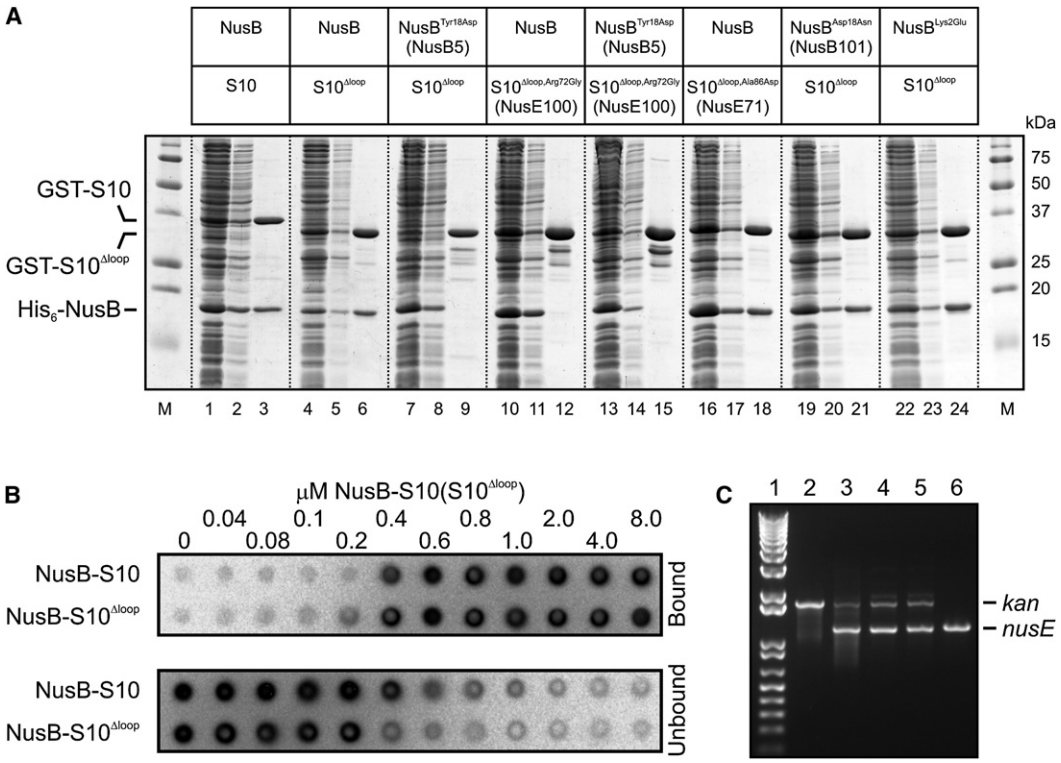

Figure 1. Analysis of the S10$^{\Delta loop}$ Mutant

(A) Copurification of GST-S10 or GST-S10$^{\Delta loop}$ and mutants with His$_6$-NusB and mutants. Groups of three lanes show the soluble extract from co-overexpression experiments (first lane), the wash (second lane), and the elution (third lane) from glutathione beads. Coexpressed proteins are indicated above the group of lanes. M, molecular mass marker.

(B) Double filter-binding assays monitoring binding of NusB-S10 complexes to an *rrn* BoxA-containing 19-mer RNA. (Upper panel) Nitrocellulose layer representing bound RNA. (Lower panel) Nylon filter representing unbound RNA. The upper lanes correspond to the full-length complex, the lower lanes to the NusB-S10$^{\Delta loop}$ complex. Numbers indicate protein concentrations in micromoles.

(C) Gel analysis of *nusE* < > *kan* recombinants. Kanamycin-resistant cells from a single colony were analyzed by PCR for configuration of the targeted chromosomal *nusE* region. Lane 1, DNA marker (Invitrogen). Lanes 2 and 3, PCR products from recombinant cells that contained pBAD*nusE*. Lanes 4 and 5, PCR products from recombinant cells that contained pBAD*nusE*$^{\Delta loop}$ initially selected either with (lanes 2 and 4) or without (lanes 3 and 5) 0.2% arabinose. Lane 6, PCR product control of WT *nusE* from the bacterial chromosome. Note that a haploid *nusE* < > *kan* knockout can be made only when pBAD*nusE* is induced by arabinose, i.e., when WT *nusE* is expressed from the plasmid (lane 2).

Presently, it is unclear how S10 is reprogrammed as a transcription factor. In particular, it is unknown how S10 interacts with NusB, whether the conformation of S10 in transcription is different from that in the 30S subunit (Gopal et al., 2001), whether the protein can remain part of the ribosome while participating in antitermination (Das et al., 1985), and why a NusB-S10 complex exhibits enhanced affinity for BoxA RNA. Here, we present genetic, biochemical, and structural data that address these questions. Our results redefine the roles of S10 and NusB during transcription regulatory processes.

RESULTS

The Long Ribosome-Binding Loop of S10 Is Dispensable for Transcriptional Functions

To investigate the structural requirements of S10 as a transcription factor, we attempted to delineate molecular regions that are dispensable for processive transcription antitermination. In the 30S subunit, S10 exhibits a globular domain that is located at the surface of the particle and an extended ribosome-binding loop that penetrates the subunit and interacts with several other r-proteins and the 16S rRNA (Schluenzen et al., 2000; Wimberly et al., 2000). We speculated that the ribosome-binding loop may be dispensable for transcription antitermination. To test this idea, we generated a truncated S10 variant in which this loop (residues 46–67) was replaced by a serine (S10$^{\Delta loop}$). To test whether the truncation affected the interaction with NusB, full-length S10 or S10$^{\Delta loop}$ was coexpressed with NusB in *E. coli* and purified via a GST-tag on the S10 molecules. Both wild-type (WT) and truncated S10 remained stably associated with NusB during purification (Figure 1A, lanes 1–6). During antitermination, the NusB-S10 complex interacts with the BoxA RNA element, a function that should be preserved in the NusB-S10$^{\Delta loop}$ complex. Indeed, the affinities of the full-length and loop-deleted complexes for BoxA-containing RNAs were comparable in a filter-binding assay (Figure 1B). We also tested the antitermination activity of the loop-deleted S10 variant directly. S10$^{\Delta loop}$ complemented λ growth at 42°C in an *E. coli*

Table 1. *nusE*$^{+}$ and *nusE*$^{\Delta loop}$ Are Dominant to *nusE71*

Chromosomal *nusE*	pBAD Plasmid	Arabinose	λ EOP
+	–	–	1
71	–	–	$<10^{-5}$
71	*nusB*$^{+}$	–	$<10^{-3}$
71	*nusE*$^{+}$	–	1.0
71	*nusE*$^{\Delta loop}$	–	1.0
71	*nusB*$^{+}$	+	$<10^{-3}$
71	*nusE*$^{+}$	+	1.0
71	*nusE*$^{\Delta loop}$	+	1.0

nusE71 is nonpermissive for λ growth at 42°C. Strains are W3102 derivatives that carry *nusE*$^{+}$ or the *nusE71* mutation in the chromosome and the indicated plasmid. λ*imm434* was titered on LB or LB plus ampicillin (50 μg/ml) at 42°C, and efficiencies of plating (EOP) were determined. Where indicated, 0.1% arabinose was added to the plate.

strain bearing a chromosomal *nusE71* defect (Table 1) that normally blocks N antitermination and λ growth at high temperatures (Friedman et al., 1981) (herein, we refer to the genes encoding S10 or S10$^{\Delta loop}$ and their variants as *nusE* or *nusE*$^{\Delta loop}$, rather than *rpsJ* or *rpsJ*$^{\Delta loop}$, respectively). Therefore, the antitermination activity of S10 is unaffected by deletion of its ribosome-binding loop.

Next, we used recombineering to ask whether *nusE*$^{\Delta loop}$ is able to suppress deletion of the chromosomal *nusE* gene, which is essential for cell growth (Bubunenko et al., 2007). In cells containing a plasmid with *nusE* under arabinose control, the chromosomal *nusE* could be replaced with a *kan* gene, conferring kanamycin resistance, in an arabinose-dependent manner (Figure 1C). In contrast, cells containing plasmid-borne *nusE*$^{\Delta loop}$ yielded only rare *nusE* < > *kan* recombinants irrespective of arabinose induction. The 40 such recombinants tested all carried an additional *nusE*$^{+}$ gene as a tandem duplicate in the chromosome. Thus, *nusE*$^{\Delta loop}$ does not encode all vital functions of *nusE*. Most likely, the flexible loop is essential for cell growth due to its role in the ribosome. These data show that transcriptional and translational functions can be partially attributed to distinct regions of S10.

Crystal Structure of a Transcriptionally Active NusB-S10 Complex

We exploited the results from the functional dissection of S10 in order to devise a high-resolution crystal structure of a transcriptionally active NusB-S10 complex. Crystals obtained from the complex of the full-length proteins did not diffract well. We reasoned that the ribosome-binding loop of S10 might be flexible off the ribosome and disturb the crystalline order. Indeed, the NusB-S10$^{\Delta loop}$ complex gave rise to crystals that diffracted to 1.3 Å resolution and allowed structure solution by molecular replacement. The structure was refined to R_{work} and R_{free} factors of 17.3% and 20.4%, respectively (see the Supplemental Data available online, Table 2).

In the structure of the complex (Figure 2A), NusB adopts an all-helical fold with two perpendicular three-helix bundles. S10$^{\Delta loop}$ exhibits a four-stranded antiparallel β sheet backed by two α helices on one side. Helix α1 and an irregular strand, β2, of

Table 2. Crystallographic Data

Data Collection	NusB-S10$^{\Delta loop}$	NusB-S10$^{\Delta loop,Ala86Asp}$
Wavelength (Å)	0.9051	0.9763
Temperature (K)	100	100
Space Group	$P2_12_12_1$	$I4_122$
Unit cell parameters (Å)	a = 40.7, b = 49.0, c = 122.8	a = b = 112.2, c = 266.2
Resolution (Å)	30.0–1.3 (1.4–1.3)[a]	50.0–2.6 (2.7–2.6)
Reflections		
Unique	56,411 (11095)	26,358 (2780)
Completeness (%)	100 (100)	100 (100)
Redundancy	15.3 (14.6)	7.1 (6.5)
I/σ (I)	17.5 (5.3)	19.8 (3.9)
R_{sym} (I)[b]	7.4 (64.8)	6.8 (46.2)
Refinement		
Resolution (Å)	20.0–1.3 (1.33–1.30)	30.0–2.6 (2.67–2.60)
Reflections		
Number	56,394 (4109)	26,337 (1921)
Completeness (%)	100 (100)	100 (100)
Test set (%)	5.0	5.0
R_{work}[c]	17.3 (27.8)	21.8 (29.5)
R_{free}[c]	20.4 (29.7)	28.0 (35.8)
Refined molecules/atoms		
Protein	1 NusB, 1 S10$^{\Delta loop}$/1779	3 NusB, 3 S10$^{\Delta loop,Ala86Asp}$/5308
Water oxygens	316	197
Solutes	3 CHES buffer molecules/39	–
Mean B factors (Å^2)		
Wilson	24.6	54.3
Protein	21.5	48.7
Water	41.0	46.0
Ligand	38.2	–
Ramachandran plot[d]		
Favored	99.1	96.8
Allowed	0.9	2.3
Outliers	0	0.9
Rmsd[e] from target geometry		
Bond lengths (Å)	0.013	0.006
Bond angles (°)	1.51	1.09
Rmsd B factors (Å^2)		
Main-chain bonds	0.86	0.28
Main-chain angles	1.31	0.51
Side-chain bonds	2.47	0.45
Side-chain angles	3.58	0.80
PDB ID	3D3B	3D3C

[a] Data for the highest resolution shell in parentheses.
[b] $R_{sym}(I) = \Sigma_{hkl}\Sigma_i|I_i(hkl) - < I(hkl) > | / \Sigma_{hkl}\Sigma_i|I_i(hkl)|$; for n independent reflections and i observations of a given reflection; < I(hkl) >, average intensity of the i observations.
[c] $R = \Sigma_{hkl}||F_{obs}| - |F_{calc}|| / \Sigma_{hkl}|F_{obs}|$; R_{work} – hkl ∉ T; R_{free} – hkl ∈ T; T, test set.
[d] Calculated with MolProbity (http://molprobity.biochem.duke.edu/).
[e] Rmsd, root-mean-square deviation.

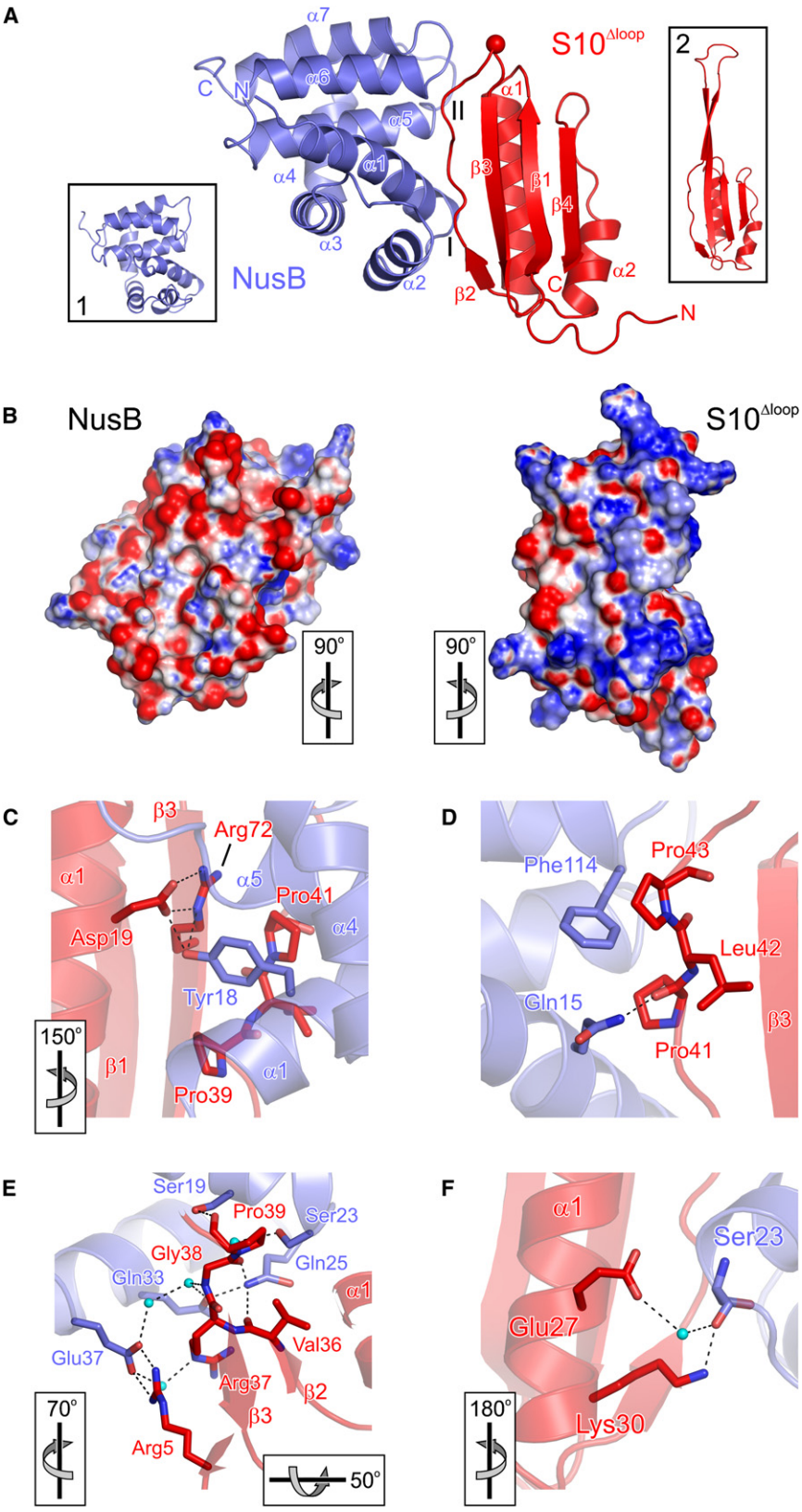

Figure 2. Structure of the NusB-S10$^{\Delta loop}$ Complex

(A) Ribbon plot of the *E. coli* NusB-S10$^{\Delta loop}$ complex. NusB, blue; S10$^{\Delta loop}$, red. Secondary structure elements and termini are labeled. The red sphere marks the site at which the ribosome-binding loop of S10 has been replaced by a single serine. (I and II) Interaction regions on the flank of the first three helix bundle (I) and on a tip of the second three helix bundle (II) of NusB. (Inset 1) NMR structure of *eco*NusB (PDB ID 1EY1; Altieri et al. [2000]) after global superpositioning on the NusB molecule of the present complex. (Inset 2) Structure of S10 from the *E. coli* 30S subunit (PDB ID 2AVY; Schuwirth et al. [2005]) after global superpositioning on the S10$^{\Delta loop}$ molecule of the present complex.

(B) Electrostatic surface potentials mapped on the surfaces of NusB (left) and S10$^{\Delta loop}$ (right) showing a view on the interfaces of both molecules. Blue, positive charge; red, negative charge. Protomers were rotated 90° relative to (A) as indicated.

(C–F) Details of the NusB-S10$^{\Delta loop}$ interaction. Interacting residues and secondary structure elements are labeled. Residues of interest are colored by atom type: carbon, the respective molecules; oxygen, red; nitrogen, blue. Cyan spheres, water molecules. Dashed lines, hydrogen bonds or salt bridges. Views relative to Figure 2A are indicated.

$S10^{\Delta loop}$ bridge the two helical bundles of NusB (contact regions I and II in Figure 2A). The region on NusB contacted by $S10^{\Delta loop}$ coincides with NusB residues that show NMR chemical shift changes upon addition of full-length S10 (Das et al., 2008). These observations further corroborate the equivalence of the WT and loop-deleted S10 in transcription.

NusB and $S10^{\Delta loop}$ approach each other via complementary electrostatic surfaces (Figure 2B), burying ~1700 $Å^2$ of combined surface area upon complex formation. The two proteins engage in mixed hydrophobic and hydrophilic interactions (Figures 2C–2F). For example, an intramolecular Asp19-Arg72 ion pair of $S10^{\Delta loop}$ forms hydrogen bonds to Tyr18 of NusB, thereby positioning Tyr18 between Pro39 and Pro41 of a proline motif (Pro39-Ile40-Pro41-Leu42-Pro43) on strand β2 of S10 (Figure 2C). The remainder of the proline motif with two intervening apolar side chains engages in snug van der Waals contacts with NusB-Phe114, sandwiching it between S10-Pro41 and S10-Pro43 (Figure 2D). Pro39 is molded into a *cis* conformation that allows it to participate in intra- and intermolecular hydrogen bonding networks (Figure 2E).

NusB and S10 Retain Their Overall Folds upon Complex Formation but Interact via Local Induced Fit

The global structures of isolated NusB (Altieri et al., 2000; Bonin et al., 2004; Das et al., 2008; Gopal et al., 2000) and of NusB in complex with $S10^{\Delta loop}$ are very similar (Figure 2A, inset 1; Table S1). $S10^{\Delta loop}$ in complex with NusB likewise resembles the structure of S10 in the 30S subunit (Schuwirth et al., 2005) (Figure 2A, inset 2; Table S1). The fold of S10 by itself is unstable (Das et al., 2008; Gopal et al., 2001); thus, NusB apparently acts to stabilize S10 in the same overall conformation it takes in the ribosome. Clearly, our data exclude the possibility that S10 is extensively remodeled by NusB as a mechanism for partitioning of S10 between the translation and transcription machineries.

While the global structures of both proteins are conserved, they are apparently adjusted by local induced fit upon complex formation. A pronounced difference to the structure of NusB determined in isolation (Altieri et al., 2000; Bonin et al., 2004; Das et al., 2008; Gopal et al., 2000) is seen in the loop connecting helices α4 and α5, which rearranges to allow an ionic interaction between NusB-Glu75 and S10-Arg16 (Figure 3A). In agreement with this observation, strong NMR chemical shift changes were previously observed in this loop of NusB upon addition of full-length S10 (Das et al., 2008). In ribosome-bound S10 (Schuwirth et al., 2005; Selmer et al., 2006; Wimberly et al., 2000), several residues that contact the 16S rRNA, including Pro39 and Arg72, have been refined with different conformations compared to the present structure of S10 in complex with NusB. While these data suggest that S10 also adjusts locally to accommodate different binding partners, the limited resolution of the ribosome structures precludes a more detailed comparison.

Binding of S10 to NusB Is Mutually Exclusive with Its Incorporation into the Ribosome and with NusB Dimerization

S10 residues His15, Arg37, Pro39, Ile40, Pro41, Pro43, Thr44, His70, and Arg72, which directly interact with NusB, also directly contact 16S rRNA in the 30S subunit (within 3.5 Å distance; Schuwirth et al. [2005]). As a consequence, the surface of S10 that binds NusB is occluded in the ribosome (Figure 3B). Thus, contrary to a previous hypothesis (Das et al., 1985; Gopal et al., 2001), S10 cannot participate with NusB in transcription antitermination as a part of the 30S subunit. This finding is in agreement with the observation that processive N-dependent antitermination can be reconstituted using purified S10 and other Nus factors (Das et al., 1985).

Mycobacterium tuberculosis NusB forms dimers (Gopal et al., 2000) whose significance for transcription antitermination has so far remained obscure. Comparison of these dimers to our NusB-$S10^{\Delta loop}$ complex shows that NusB dimerization would interfere with S10 binding (Figure 3C). This observation is in agreement with our previous suggestion (Bonin et al., 2004) that dimerization may be used as a packaging mechanism by some organisms to downregulate aberrant activities of isolated NusB. Similar autoinhibitory mechanisms have been demonstrated for other transcription antitermination factors (Belogurov et al., 2007; Mah et al., 2000).

Molecular Basis of the *nusB5* and *nusE100* Phenotypes

Mutations in *nusB* and *nusE* have served as important genetic tools to study processive antitermination. However, the biochemical basis for the dysfunction or suppressor activity of any of the mutant proteins was not defined. The *nusB5* allele gives rise to a Tyr18Asp mutation in NusB (Court et al., 1995) and leads to a defect in N-dependent antitermination that blocks λ growth (Friedman et al., 1976). The *nusE100* mutation restricts Nun termination but not N antitermination (Robledo et al., 1991). We have sequenced the *nusE100* allele and find that it encodes an $S10^{Arg72Gly}$ variant. Remarkably, NusB-Tyr18 and S10-Arg72 are both involved in the same buried, hydrophilic, intermolecular interaction network at the center of the NusB-S10 interface (Figure 2C). Replacement of NusB-Tyr18 by Asp or replacement of S10-Arg72 by Gly is expected to interfere with this interaction network. Therefore, it is possible that the defects of the mutant alleles are in part caused by a weakened NusB-S10 affinity. We tested this idea by monitoring the ability of the mutant proteins to sustain NusB-S10 interaction in GST-pull-down assays. Indeed, the NusB5 variant (Tyr18Asp) did not bind to $S10^{\Delta loop}$ (Figure 1A, lanes 7–9), and the $S10^{\Delta loop,Arg72Gly}$ mutant protein of $nusE100^{\Delta loop}$ failed to interact with NusB (lanes 10–12).

Previously, the lack of production of a stable gene product was thought to be the cause of the *nusB5* defect in N antitermination (Mason et al., 1992). Our results, in contrast, suggest that *nusB5* gives rise to a gene product that is less active due to a weakened interaction with S10. In that case, the *nusB5* defect may be overcome simply by mass action. Therefore, we asked if high levels of NusB5 can restore N antitermination. Indeed, overexpression of the NusB5 protein in an *E. coli nusB* deletion strain partially rescued λ growth (Table S2). In agreement with this observation, multiple copies of a plasmid carrying the *nusB5* gene have previously been found to complement a chromosomal *nusB5* allele (Court et al., 1995). Thus, our data underscore the importance of a stable NusB-S10 interaction at physiological expression levels of these proteins for N and Nun activities.

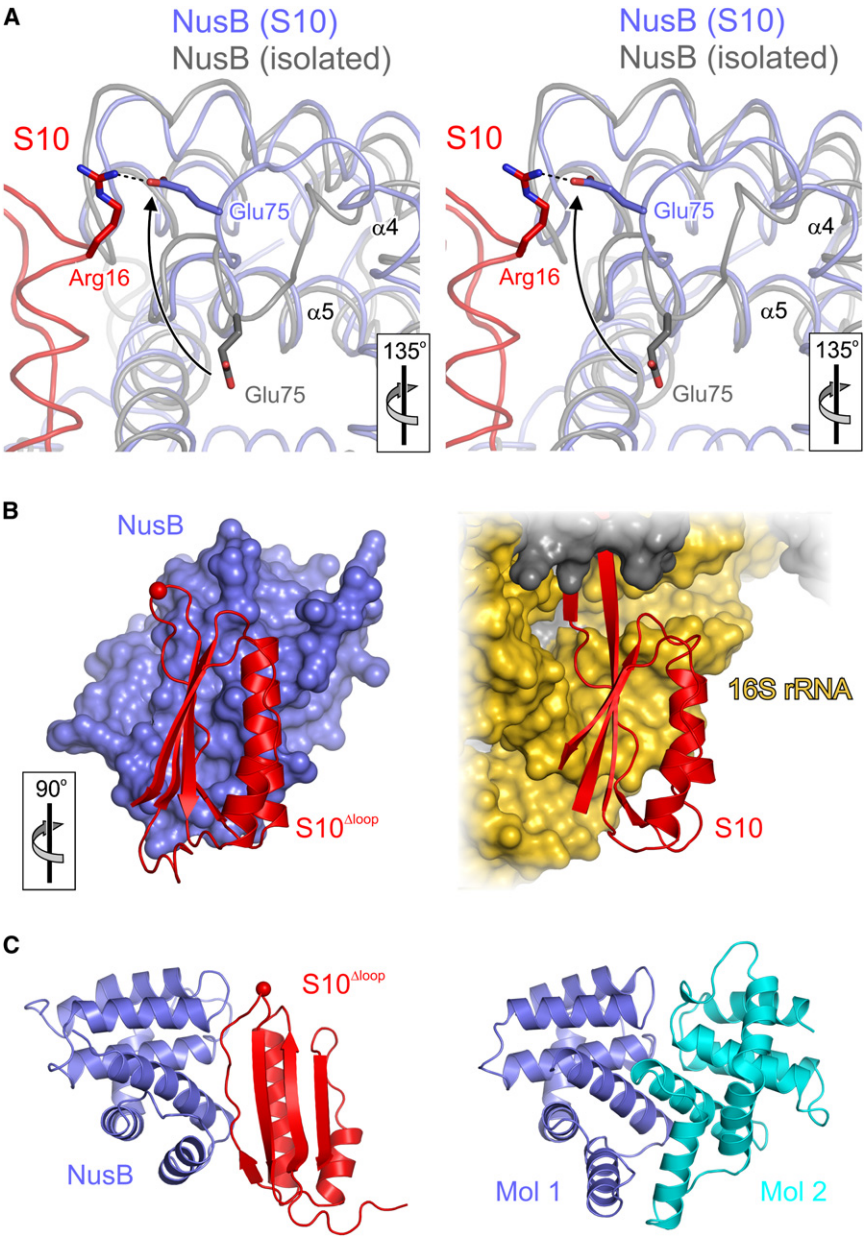

Figure 3. Aspects of the NusB-S10$^{\Delta loop}$ Interaction

(A) Stereo ribbon plot showing induced-fit adjustment of the loop between helices α4 and α5 in NusB. An NMR structure of *E. coli* NusB (gray, PDB ID 1EY1; Altieri et al. [2000]) was superimposed on the NusB subunit of the present NusB-S10$^{\Delta loop}$ complex (blue and red, respectively). The view relative to Figure 2A is indicated. Glu75 of NusB changes its position upon complex formation (arrow) in order to engage in a salt bridge with Arg16 of S10$^{\Delta loop}$. Relevant residues are in sticks and colored by atom type as before.

(B) Comparison of S10$^{\Delta loop}$ (red) binding to NusB (blue) and S10 binding to the remainder of the 30S subunit (rRNA, gold; r-proteins, gray). The orientation relative to Figure 2A is indicated.

(C) Comparison of the present NusB-S10$^{\Delta loop}$ complex (blue and red, left) with the *M. tuberculosis* NusB dimer (blue and cyan, right; PDB ID 1EYV; Gopal et al. [2000]). The blue NusB molecules of both complexes are in the same orientation.

The NusB-S10 Complex Exhibits an Intermolecular, Mosaic, and Contiguous BoxA RNA-Binding Surface

To explore the mechanism by which S10 enhances the affinity of NusB for BoxA RNA, we investigated how NusB and the NusB-S10 complex interact with BoxA-containing RNA. We exposed NusB-RNA or NusB-S10-RNA complexes to UV light and analyzed by mass spectrometry the zero-length crosslinks generated (Table S3; Figure S1). We employed the same two 19 nt λ NutR BoxA or *rrn* BoxA RNAs, previously used in fluorescence-based interaction studies (Greive et al., 2005) (see Figure 4A). Overall, we identified four peptides in NusB (B1, B1′, B2, and B3) and three in full-length S10 (E1, E2, and E3) that crosslinked to distinct, short RNA elements (Figure 4A; Table S3). UV-induced crosslinking in the absence of RNA oligos and mass analysis with complete mixtures but without UV irradiation did not give rise to any peaks corresponding to those of the identified peptide-RNA crosslinks.

Scrutinizing the sequences of the crosslinked peptides and RNA elements allowed us to deduce unequivocally the molecular neighborhoods (Supplemental Results and Discussion). These data show that NusB is in close proximity to residues 3–8 of *rrn* BoxA and residues 3–9 of λ BoxA, while S10 is in direct contact with residues 8, 9, and 12 of *rrn* BoxA; residues 7, 8, and 12 of λ BoxA; and residues just downstream in either of the RNAs (Figure 4A; Table S3). The BoxA positions in direct contact with NusB and S10 are remarkably congruent with residues 2–9 of *rrn* BoxA and residues 2–7 of λ BoxA, which are essential for recruitment of NusB and S10 to the antitermination machineries (Mogridge et al., 1998). In addition, parts of the S10 ribosome-binding loop (the entire peptide E2 and part of E3) crosslinked to RNA at the very 3′ end of the core BoxA elements and to nucleotides immediately downstream (Figure 4A; Table S3). Thus, the ribosome-binding loop fosters auxiliary, but not essential (Table 1), mRNA contacts that might enhance processive antitermination.

Since we find virtually identical crosslinks of NusB to the RNAs in the absence or in the presence of S10 (Table S3), we conclude that the specificity of the NusB-BoxA RNA contacts is influenced little if at all by S10. Thus, the direct S10-BoxA interactions detected herein are responsible for the increased BoxA RNA affinity of the NusB-S10 complex compared to NusB alone. Since isolated S10 binds RNA weakly and largely nonspecifically (Greive et al., 2005), NusB apparently stabilizes an RNA-binding

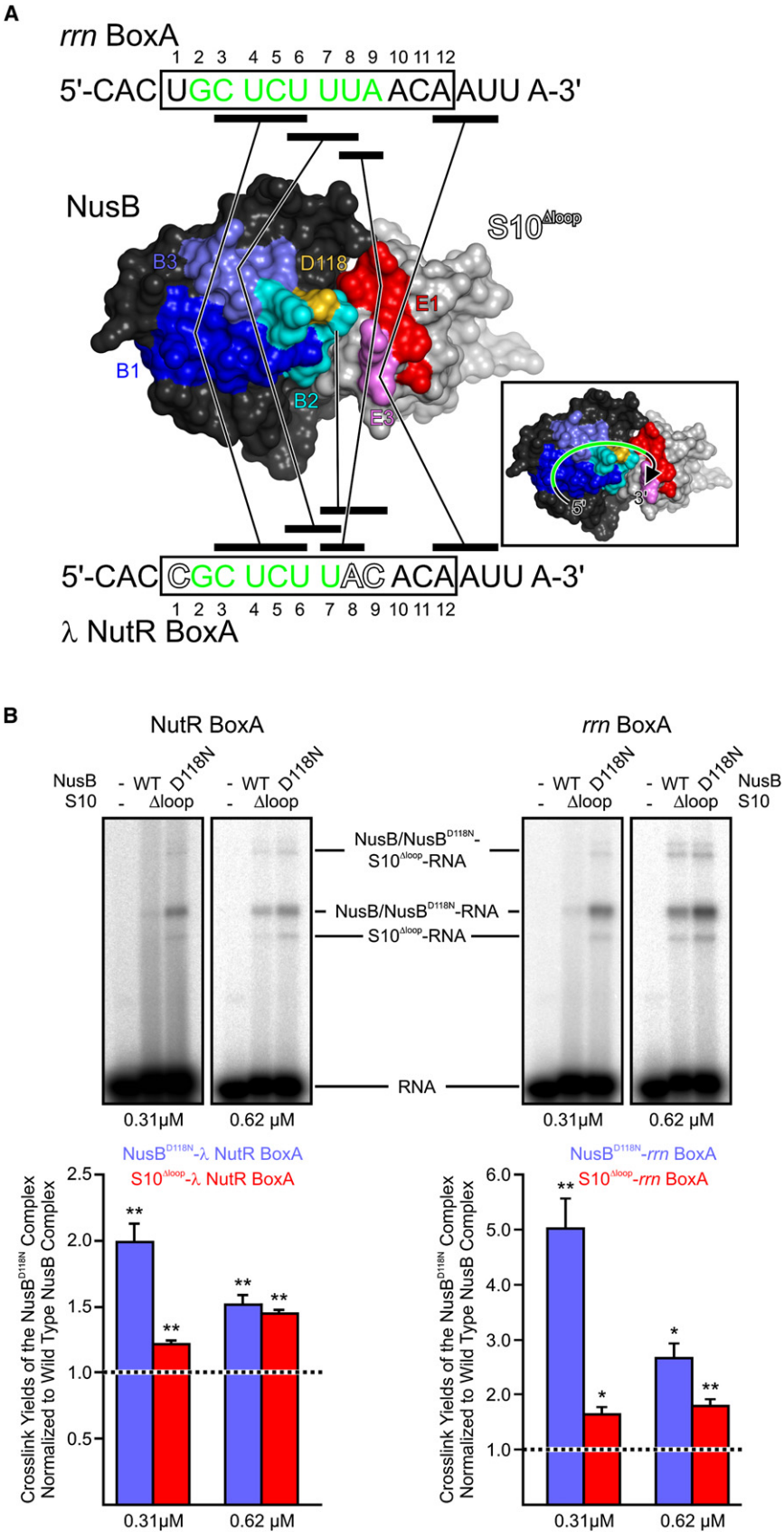

Figure 4. BoxA RNA Binding

(A) Mapping of crosslinked peptides on the surface of the NusB-S10$^{\Delta loop}$ complex. The view is from the top of Figure 2A. NusB, dark gray; S10, light gray. Crosslinked peptides of NusB (B1, B2, B3; see Table S3 for peptide sequences) are dark blue, cyan, and steel blue, respectively. Crosslinked peptides of S10 (E1 and E3) are red and violet, respectively. Asp118, gold. RNAs encompassing the *rrn* and λ BoxA elements and used for crosslinking are given above and below the structure, respectively. Boxed regions with residue numbers indicate the core BoxA elements. Residues in green of *rrn* BoxA RNA and λ BoxA RNA have previously been implicated in recruitment of NusB and S10 to antitermination complexes by mutational analysis (Mogridge et al., 1998). Outlined residues differ in λ BoxA compared to *rrn* BoxA. Black bars designate crosslinked regions of the RNAs. They are connected by lines to the peptides, to which they have been crosslinked (Table S3). Inset 1 illustrates the deduced topology of the NusB-S10-BoxA RNA complexes.

(B) (Top) Representative crosslinking of λ NutR BoxA RNA (left two panels) or *rrn* BoxA RNA (right two panels) to NusB-S10$^{\Delta loop}$ or NusB101-S10$^{\Delta loop}$ (NusB^{Asp118Asn}-S10$^{\Delta loop}$). Two concentrations of protein complex (0.31 and 0.62 μM) were crosslinked, resolved on SDS gels, and visualized by autoradiography. In each panel, RNA alone is in the left lane, NusB-S10$^{\Delta loop}$ complex in the central lane, and NusB101-S10$^{\Delta loop}$ complex in the right lane. (Bottom) Quantification of crosslink yields. Values are the crosslink yields of the protein components of the NusB101-S10$^{\Delta loop}$ samples, relative to the crosslink yields of the corresponding components of the NusB-S10$^{\Delta loop}$ samples. The crosslink yields of the components of the NusB-S10$^{\Delta loop}$ samples were set at 100% (dashed lines). Values represent the mean of three independent experiments ± the standard errors of the mean. *p ≤ 0.032; **p ≤ 0.020.

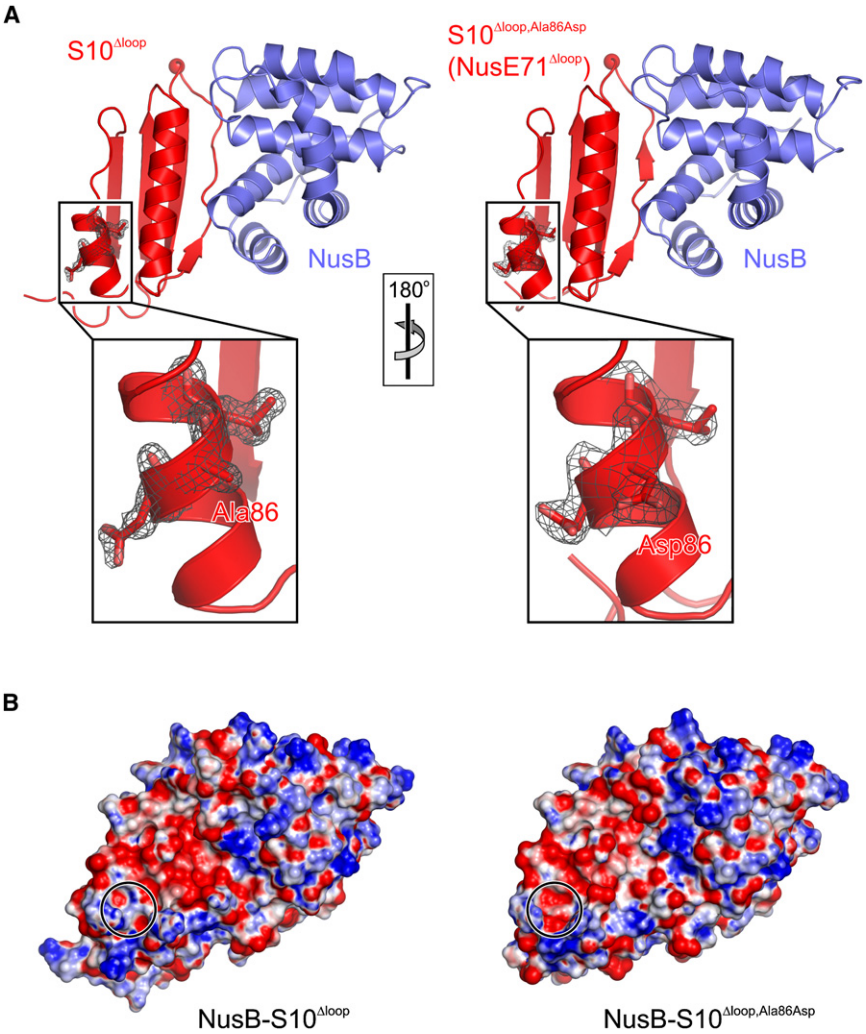

Figure 5. NusB-S10$^{\Delta loop,Ala86Asp}$ Complex

(A) Comparison of the NusB-S10$^{\Delta loop}$ complex (left) with the NusB-S10$^{\Delta loop,Ala86Asp}$ complex (right). Gray meshes, final $2F_o - F_c$ electron densities covering residue 86 and neighboring residues of the S10$^{\Delta loop}$ molecules, contoured at the 1σ level. (Insets) Closeup views of the residue 86 regions. The orientation relative to Figure 2A is indicated.

(B) Comparison of the electrostatic surface potentials of the complexes. Blue, positive charge; red, negative charge. Left, NusB-S10$^{\Delta loop}$ complex. Right, NusB-S10$^{\Delta loop,Ala86Asp}$ complex. The positions of residue 86 are circled. The orientations are the same as in (A).

conformation of S10 and positions S10 on the BoxA RNA, suggesting that NusB loads S10 onto a specific RNA element.

The amino acid residues crosslinked to RNA in both NusB and S10 are dispersed in the primary sequences but nevertheless coalesce in 3D on one surface of the NusB-S10$^{\Delta loop}$ complex (Figure 4A). Peptides B1 (B1′), B2, and B3 form a contiguous surface on NusB, and peptide E1 of S10 directly neighbors the C terminus of peptide E3 at the base of the ribosome-binding loop. The tip of NusB peptide B2 is in weak direct contacts with S10 peptides E1 and E3 (Figure 4A). Thus, NusB and S10 together present a contiguous, mosaic BoxA-binding surface. We combined the results from our structural and crosslinking analyses to derive the overall topology of the NusB-S10-RNA complex (Figure 4A, inset). The central region of a BoxA element is placed on the confluent binding surface of the protein complex. The RNA runs 5′ to 3′ from the NusB to the S10 RNA-binding patches.

nusB101 Represents a Gain-of-Function Mutation with Increased RNA Affinity

The *nusB101* mutation (Asp118Asn) suppresses the N antitermination defects of NusA1 and NusE71 mutants at high temperatures (Ward et al., 1983). Notably, NusB-Asp118 is part of peptide B2, which lies at the center of the closely spaced RNA-binding patches on NusB and S10 (Figure 4A). Removal of a negative charge at the NusB-118 position could conceivably increase the RNA affinity of NusB and of the NusB-S10 complex, in agreement with a previous proposal (Court et al., 1995). We tested this idea by crosslinking increasing amounts of NusB-S10$^{\Delta loop}$ and of NusB101-S10$^{\Delta loop}$ (NusB^{Asp118Asn}-S10$^{\Delta loop}$) to BoxA-containing RNAs under conditions in which the crosslink yields reflect the binding equilibria. As predicted, NusB101-S10$^{\Delta loop}$ exhibited increased affinities for either λ or *rrn* BoxA sequences (Figure 4B; Figure S2). Since both NusB101 and S10 showed increased crosslinking, the difference was not due to direct crosslinking of Asn118 of NusB101 to the RNA. Thus, *nusB101* represents a gain-of-function mutation that increases the affinity of NusB for BoxA. Consistent with cooperativity among the component antitermination factors, enhanced RNA affinity in NusB101 might compensate for decreased RNA affinity of the suppressed NusA1 mutant, in which a core residue of the S1 RNA-binding domain is altered (Worbs et al., 2001).

The *nusE71* Mutation Defines an Additional Interaction Surface on S10

The residue affected by the *nusE71* mutation (Ala86Asp), which blocks both N and Nun, is remote from the NusB interface and the RNA-binding region of S10. We have determined the structure of a NusB-S10$^{\Delta loop,Ala86Asp}$ complex and find that it is virtually identical to the WT complex (root-mean-square deviation of ~0.8 Å for 206 Cα atoms; Table 2; Figure 5A). Therefore, dysfunction of S10^{Ala86Asp} is not due to a global effect on the structure of the protein. Rather, the mutation changed the local surface properties of S10 (Figure 5B). This finding suggests that yet another molecular interaction of S10 may be attenuated in S10^{Ala86Asp}. S10 is known to interact directly with RNAP

(Mason and Greenblatt, 1991), and it is possible that the helix α2 region encompassing residue 86 is involved in this association. Alternatively, the S10 region around Ala86 might mark an interface with N and Nun; N and S10 proteins are reported to copurify in some preparations (Mogridge et al., 1995, 1998). This notion would explain the otherwise puzzling observation that *nusE71* does not block *rrn* antitermination, which uses RNAP but not N or Nun (Zellars and Squires, 1999).

S10 Supports Transcription Antitermination in the Absence of NusB

N and *rrn* antitermination and Nun termination involve appropriate tethering of BoxA and BoxB RNA sites to RNAP via N or Nun and the Nus factors (Nodwell and Greenblatt, 1991). Since S10 directly contacts RNA (this work) and RNAP (Mason and Greenblatt, 1991), we considered the possibility that S10 may be the functional antitermination factor in the NusB-S10 complex at Nut sites. To test this idea, we overexpressed S10 and $S10^{\Delta loop}$ in an *E. coli* strain lacking the *nusB* gene. Strikingly, overexpression of either S10 or $S10^{\Delta loop}$ rescued λ growth, restoring functional N antitermination in the absence of NusB (Table 3). Similarly, S10 or $S10^{\Delta loop}$ expression rescued Nun-dependent termination in the *nusB*-deletion strain, as determined by the expression of a *lacZ* gene promoter-distal to λ Nut (Table 3). These results are at variance with the traditional view that the role of S10 is to recruit NusB to RNAP (Mason and Greenblatt, 1991; Mason et al., 1992). We propose, therefore, that NusB, although it engages in more extensive BoxA contacts than S10, merely serves as a loading factor that ensures efficient entry of S10 into these transcription complexes, while S10 constitutes the critical antitermination component of the NusB-S10 complex.

Table 3. Overproduction of S10 or $S10^{\Delta loop}$ Restores λN and HK022 Nun Functions in a Δ*nusB* Strain

N Antitermination			
Chromosomal *nusB*	pBAD Plasmid	Arabinose	λ EOP
+	–	–	1.0
Δ	–	–	<10−5
Δ	$nusE^{+}$	–	<10−2
Δ	$nusE^{\Delta loop}$	–	<10−2
Δ	$nusE^{+}$	+	0.30
Δ	$nusE^{\Delta loop}$	+	0.71
Nun Termination			
HK022	pBAD	−Arabinose	+Arabinose
–	*nusE*	2260	1453
–	$nusE^{\Delta loop}$	2373	1856
+	*nusE*	951 (58)	213 (85)
+	$nusE^{\Delta loop}$	1208 (49)	406 (78)

N antitermination, $nusE^{+}$ and $nusE^{\Delta loop}$ were carried by a pBAD plasmid and, where indicated, induced with 0.1% arabinose. λ*imm434*, which is insensitive to λ repressor, was plated at 37°C on LB plates with or without (+/−) 50 μg/ml ampicillin to determine EOP. Strains are W3102 derivatives carrying the fusion λ*cI857* − *pR* − *cro* (ΔRBS) − *nutR* − *tR1* − *cII::lacZ*. Nun termination, *nusB::Cam* cells additionally carried a HK022 prophage as indicated. Cells were grown at 37°C until early log phase and then shifted to 42°C for 2 hr without ("−Arabinose") or with ("+Arabinose") 0.1% arabinose. Numbers in parentheses indicate percent termination.

DISCUSSION

The balance between transcription termination and progression of transcription (antitermination) is controlled at specific sites in genes. Factor ensembles that interact with RNAP have evolved to interpret such control sites. One example is the antitermination machinery that regulates the transcription of the phage λ genome and of rRNA genes in bacteria. The molecular mechanisms underlying this fundamental regulatory principle of transcription are incompletely understood. Here, we have presented work that redefines the roles of an r-protein, S10, which is part of these antitermination complexes, and of another antitermination factor, NusB, which forms a stable subcomplex with S10. Apart from the implications for a fundamental transcription regulatory principle, our results have repercussions for the generation of functional diversity in proteomes by employing one protein, S10, for multiple activities.

$S10^{\Delta loop}$ Is a Tool to Dissect Translational and Transcriptional Functions of S10

We have delineated structural elements of S10 that are exclusively required for S10 function in the ribosome but not in transcription. Our finding that the long loop of S10 is dispensable in transcription is consistent with the observation that mutants defective in transcriptional functions (*nusE71*, *nusE100*) map to the globular part of S10. The functional architecture of S10 is paralleled by that of r-protein L4, which also has a second activity as a transcriptional attenuator (Lindahl et al., 1983). In L4, a similar ribosome-binding loop was also found dispensable for attenuation (Worbs et al., 2000; Zengel et al., 2003). Our findings show that evolution made economic use of r-proteins by diverting regions not under strict selection by ribosomal functions to other purposes.

The S10 loop is of obvious architectural importance for the 30S subunit (Schluenzen et al., 2000; Wimberly et al., 2000), consistent with our observation that the loop is essential for cell viability. These results suggest that the transcription antitermination activity of S10 is independent of ribosomes or ribosome-bound S10, in agreement with our finding that S10 cannot bind to NusB and the 30S subunit at the same time. The above results also suggest that under normal growth conditions, rRNA transcription antitermination is not essential and that proteins involved in antitermination are required because of their role in other cellular processes, as recently also shown for other antitermination factors (Bubunenko et al., 2007; Phadtare et al., 2007).

S10 Is Adapted to Different Functional Contexts without Global Structural Remodeling

Since its fold is unstable, S10 has been suggested to represent a largely intrinsically unstructured protein, whose structure could adapt to different functional contexts (Gopal et al., 2001). S10 expressed alone exhibits low solubility and tends to aggregate. NusB confers increased solubility on S10 (Figure 1A), suggesting that S10 may preferentially exist in complex with NusB off the

ribosome. We observe that the bulk of S10 adopts the same global fold in complex with NusB as in the ribosome. Thus, our results rigorously exclude the possibility that the structure of S10 is extensively remodeled in order to recruit the protein as a transcription factor. Indeed, the long ribosome-binding loop is most likely the only intrinsically unfolded region of S10.

Mutually Exclusive Binding of S10 to the 30S Subunit or NusB May Provide for Feedback Control of Ribosome Biogenesis

Balancing the levels of ribosomal building blocks is critical for bacteria, since ribosome biosynthesis can consume half of the available metabolic energy (Bremer and Dennis, 1987). A number of negative feedback loops have been characterized that act to ensure stoichiometric levels of ribosomal constituents. When expressed in surplus of their rRNA-binding sites, several r-proteins restrict their own expression and that of other proteins in their operons by binding to their own mRNAs, thereby sequestering the messages from translation (Lindahl and Zengel, 1986). In addition to such translational feedback, r-protein L4 also downregulates transcription of its operon (Lindahl et al., 1983). Evidence presented here suggests that such negative feedback may be complemented by positive feedback through r-protein S10. Since crystal structures show that S10 cannot participate in transcription antitermination on RNAP and translation on the ribosome at the same time, only S10 produced in excess of ribosomes will elicit antitermination of *rrn* operons and thus a higher rate of rRNA biosynthesis. As a consequence, surplus S10 would act to increase rRNA levels. With respect to rRNA production, NusB and BoxA may therefore be envisioned as enhancers of an S10-based feedback regulation.

S10 and NusB Form a Functional Module for Recognition of BoxA

Much of the proteome is organized as functional modules (Hartwell et al., 1999), which support an autonomous function as, for example, devices within a macromolecular machine. Here we show how the NusB-S10 complex acts as a functional RNA-binding module of the transcriptional machineries with which it is associated. We find that both subunits of the NusB-S10 complex contribute to a mosaic yet contiguous binding surface for a crucial RNA signaling element, BoxA. An analogous situation was encountered intramolecularly in NusA, in which different RNA-binding domains come together to create an enlarged, composite RNA-binding site (Beuth et al., 2005; Worbs et al., 2001). Cooperation between two or more subunits to generate a composite binding surface for an additional factor is an important architectural principle in macromolecular assemblies (Liu et al., 2007).

A Shift in Paradigm: S10 Is the Active Antitermination Factor of the NusB-S10 Complex

In the traditional view of processive antitermination, S10 serves as an auxiliary factor that recruits the antitermintion factor NusB to RNAP (Mason and Greenblatt, 1991; Mason et al., 1992). Contrary to that view, we show that S10 supports N antitermination and Nun termination even in the absence of NusB. According to our work, NusB has supportive functions, while the fundamental antitermination activity of the complex relies on S10. What are the supportive functions of NusB, and what constitutes the fundamental antitermination activity of S10?

S10 is a truly multifunctional protein even within transcriptional complexes. Apart from interacting with NusB (Mason et al., 1992; and this work), it directly binds RNAP (Mason and Greenblatt, 1991). Furthermore, S10 has been suggested to contact phage λ protein N (Mogridge et al., 1995, 1998). Our work shows that S10 is even more versatile and also binds to the BoxA RNA element. Thus, S10 constitutes a hub within the N and *rrn* antitermination and Nun termination complexes, through which the functions of other factors may be integrated. However, isolated S10 binds RNA with low specificity (Greive et al., 2005). Under physiological conditions, positioning of S10 on the mRNA by RNAP or the phage proteins is presumably inefficient. NusB is therefore required as an adaptor that ensures efficient loading of S10 on the nascent RNA at BoxA and subsequent contact with RNAP.

EXPERIMENTAL PROCEDURES

Details of molecular biology, protein production, GST pull-down, filter binding, and crystallographic procedures are given in the Supplemental Experimental Procedures.

Gene Essentiality Assay

The functionality of the $S10^{\Delta loop}$ mutant for cell growth was analyzed using a gene essentiality assay based on recombineering (Bubunenko et al., 2007), as recently described for IF1 mutants (Phadtare et al., 2007). Briefly, recombinogenic DY330 cells containing the *λ red* genes were transformed with pBAD plasmids expressing either $S10^{\Delta loop}$ or WT S10 as a positive control. Cells were then subjected to recombineering to replace the chromosomal *nusE* open reading frame by fusing its first 15 codons to the *kan* open reading frame ($nusE_{15}$-*kan*). The *kan* PCR fragment amplified for recombineering was flanked with *nusE* homologous regions using primers 5′-**ATGCAGAACCAAAGAATCCGTATCCGCCTGAAAGCGTTTGATCAT**ATTGAACAAGATGGATTGCACGC and 5′-**CAATCATTGTTTCAACCTCTCAATCGCTCAATGACCTGA**TCAGAAGAACTCGTCAAGAAG (*nusE* regions in bold). Recombinants were selected on L plates with 25 μg/ml kanamycin and with or without 0.2% arabinose. Kanamycin-resistant recombinants were analyzed by PCR for the configuration of the targeted *nusE* chromosomal region using a pair of primers flanking the *nusE* gene: 5′-TAGCCGAATTTGGCTACCTAACAAT and 5′-GAAGGTAGTTTCGGAAACAGTCAG. The appearance of a single *nusE* < > *kan* fragment indicates that S10 expressed from a plasmid is functional and is able to complement the nonviable chromosomal *nusE* knockout (Bubunenko et al., 2007). The appearance of two fragments representing *nusE* < > *kan* and *nusE* indicates that the $S10^{\Delta loop}$ copy expressed from a plasmid is not functional and is unable to complement a chromosomal *nusE* knockout. Thus, in this case, recombinants are rare and have a knockout copy and a WT copy of *nusE*, which reflects the special diploid nature of these strains (Bubunenko et al., 2007).

UV-Induced Crosslinking Assay

Varying concentrations (0, 0.15, 0.31, 0.62, 1.25, and 2.5 μM) of NusB-$S10^{\Delta loop}$ or NusB101-$S10^{\Delta loop}$ ($NusB^{Asp118Asn}$-$S10^{\Delta loop}$) were mixed with [^{32}P]-labeled RNA oligonucleotide in 10 μl reaction volumes and exposed to 254 nm UV light for 5 min at 4°C (Lingel et al., 2003). Reactions were analyzed by 15% SDS PAGE. Gels were dried and developed on a phosphoimager. Under saturating conditions, a maximum of ~7% of the total radioactivity was shifted on gels. For quantification, 0.31 and 0.62 μM of NusB-$S10^{\Delta loop}$ or NusB101-$S10^{\Delta loop}$ were crosslinked as above. Crosslinked samples from three independent experiments were analyzed on the same SDS gel. For loading control, each sample was divided and averaged. Radiolabeled bands were quantified by densitometry using ImageQuant software (GE Healthcare). Crosslink yields

for the components of the WT NusB-based complex were normalized to 1, and the yields for the corresponding components of the $NusB^{Asp118Asn}$-based complex were represented relative to the WT sample.

Mass Spectrometric Analysis of UV-Induced Crosslinking Sites

RNA oligomer (8 nmole) was incubated with 4 nmole of recombinant NusB or NusB-S10 complex in 300 μl of crystallization buffer and exposed to 254 nm UV light for 5 min at 4°C. Crosslinked samples were precipitated with three volumes of ethanol, dried in a speed vac, and dissolved in 50 mM Tris-HCl (pH 7.9), 4 M urea. The urea concentration was adjusted to 1 M, and the RNA oligonucleotides were hydrolyzed with 1 μg each of RNases A and T1 for 2 hr at 52°C. Trypsin was added to a final ratio of 1:20 (enzyme:substrate) prior to overnight incubation at 37°C.

The samples were desalted and enriched for crosslinks using TiO_2 microcolumns generated in-house and injected onto a nano-liquid chromatography (nanoLC) system (Agilent) equipped with a C18 trapping column (Maisch) in line with an analytical C18 column (200 × 0.075 mm) packed in-house. nanoLC separation and electrospray ionization-tandem mass spectrometry were performed with a Q-ToF Ultima mass spectrometer (Waters) as described elsewhere (Deckert et al., 2006).

ACCESSION NUMBERS

Coordinates and structure factors have been deposited with the RCSB Protein Data Bank (http://www.rcsb.org/pdb/) under accession codes 3D3B (NusB-$S10^{\Delta loop}$) and 3D3C (NusB-$S10^{\Delta loop,\ Ala86Asp}$).

SUPPLEMENTAL DATA

The Supplemental Data include Supplemental Experimental Procedures, Supplemental Results and Discussion, Supplemental References, three tables, and two figures and can be found with this article online at http://www.molecule.org/supplemental/S1097-2765(08)00808-3.

ACKNOWLEDGMENTS

We thank Elke Penka and Monika Raabe (Max-Planck-Institute for Biophysical Chemistry, Göttingen, Germany) for excellent technical assistance, the staff at beamlines PXI/II (SLS, Villigen, Switzerland) and BL14.2 (BESSY, Berlin, Germany) for support during diffraction data collection, and Andrew Byrd and Amanda Altieri (NCI, Frederick, MD, USA) for communication of results prior to publication. M.C.W. was supported by grant WA 1126/3-1 from the Deutsche Forschungsgemeinschaft. M.E.G. was supported by National Institutes of Health (NIH) grant GM37219. H.U. was supported by a young investigator grant of EURASNET. This research was supported in part by the Intramural Research Program of the NIH, National Cancer Institute, Center for Cancer Research, and by a Trans NIH/FDA Intramural Biodefense Program Grant from NIAID to D.L.C. This project was funded in part with federal funds from the National Cancer Institute, National Institutes of Health, under contract N01-CO-12400. The content of this publication does not necessarily reflect the views or policies of the Department of Health and Human Services, nor does mention of trade names, commercial products, or organizations imply endorsement by the U.S. government. The authors declare that they have no competing financial interests.

Received: June 30, 2008
Revised: September 24, 2008
Accepted: October 21, 2008
Published: December 24, 2008

REFERENCES

Altieri, A.S., Mazzulla, M.J., Horita, D.A., Heath Coats, R., Wingfield, P.T., Das, A., Court, D.L., and Byrd, A.R. (2000). The structure of the transcriptional antiterminator NusB from Escherichia coli. Nat. Struct. Biol. *7*, 470–474.

Belogurov, G.A., Vassylyeva, M.N., Svetlov, V., Klyuyev, S., Grishin, N.V., Vassylyev, D.G., and Artsimovitch, I. (2007). Structural basis for converting a general transcription factor into an operon-specific virulence regulator. Mol. Cell *26*, 117–129.

Berg, K.L., Squires, C., and Squires, C.L. (1989). Ribosomal RNA operon antitermination. Function of leader and spacer region box B-box A sequences and their conservation in diverse micro-organisms. J. Mol. Biol. *209*, 345–358.

Beuth, B., Pennell, S., Arnvig, K.B., Martin, S.R., and Taylor, I.A. (2005). Structure of a Mycobacterium tuberculosis NusA-RNA complex. EMBO J. *24*, 3576–3587.

Bonin, I., Robelek, R., Benecke, H., Urlaub, H., Bacher, A., Richter, G., and Wahl, M.C. (2004). Crystal structures of the antitermination factor NusB from Thermotoga maritima and implications for RNA binding. Biochem. J. *383*, 419–428.

Bremer, H., and Dennis, P.P. (1987). Modulation of chemical composition and other parameters of the cell by growth rate. In *Escherichia coli* and *Salmonella thyphimurium*: Cellular and Molecular Biology, F.C. Neidhardt, J.L. Ingraham, K.B. Low, B. Magasanik, M. Schaechter, and H.E. Umbarger, eds. (Washington, DC: American Society for Microbiology), pp. 1527–1542.

Bubunenko, M., Baker, T., and Court, D.L. (2007). Essentiality of ribosomal and transcription antitermination proteins analyzed by systematic gene replacement in Escherichia coli. J. Bacteriol. *189*, 2844–2853.

Court, D.L., Patterson, T.A., Baker, T., Costantino, N., Mao, X., and Friedman, D.I. (1995). Structural and functional analyses of the transcription-translation proteins NusB and NusE. J. Bacteriol. *177*, 2589–2591.

Das, A., Ghosh, B., Barik, S., and Wolska, K. (1985). Evidence that ribosomal protein S10 itself is a cellular component necessary for transcription antitermination by phage lambda N protein. Proc. Natl. Acad. Sci. USA *82*, 4070–4074.

Das, R., Loss, S., Li, J., Waugh, D.S., Tarasov, S., Wingfield, P.T., Byrd, R.A., and Altieri, A.S. (2008). Structural biophysics of the NusB:NusE antitermination complex. J. Mol. Biol. *376*, 705–720.

Deckert, J., Hartmuth, K., Boehringer, D., Behzadnia, N., Will, C.L., Kastner, B., Stark, H., Urlaub, H., and Lührmann, R. (2006). Protein composition and electron microscopy structure of affinity-purified human spliceosomal B complexes isolated under physiological conditions. Mol. Cell. Biol. *26*, 5528–5543.

Friedman, D.I., and Court, D.L. (1995). Transcription antitermination: the lambda paradigm updated. Mol. Microbiol. *18*, 191–200.

Friedman, D.I., and Gottesman, M.E. (1983). Lytic mode of lambda development. In Lambda II, R.W. Hendrix, J.W. Roberts, F.W. Stahl, and R.A. Weisberg, eds. (Cold Spring Harbor, NY: Cold Spring Harbor Laboratory Press), pp. 21–51.

Friedman, D.I., Baumann, M., and Baron, L.S. (1976). Cooperative effects of bacterial mutations affecting lambda N gene expression. I. Isolation and characterization of a nusB mutant. Virology *73*, 119–127.

Friedman, D.I., Schauer, A.T., Baumann, M.R., Baron, L.S., and Adhya, S.L. (1981). Evidence that ribosomal protein S10 participates in control of transcription termination. Proc. Natl. Acad. Sci. USA *78*, 1115–1118.

Gopal, B., Haire, L.F., Cox, R.A., Jo Colston, M., Major, S., Brannigan, J.A., Smerdon, S.J., and Dodson, G. (2000). The crystal structure of NusB from Mycobacterium tuberculosis. Nat. Struct. Biol. *7*, 475–478.

Gopal, B., Papavinasasundaram, K.G., Dodson, G., Colston, M.J., Major, S.A., and Lane, A.N. (2001). Spectroscopic and thermodynamic characterization of the transcription antitermination factor NusE and its interaction with NusB from *Mycobacterium tuberculosis*. Biochemistry *40*, 920–928.

Greive, S.J., Lins, A.F., and von Hippel, P.H. (2005). Assembly of an RNA-protein complex. Binding of NusB and NusE (S10) proteins to boxA RNA nucleates the formation of the antitermination complex involved in controlling rRNA transcription in Escherichia coli. J. Biol. Chem. *280*, 36397–36408.

Hartwell, L.H., Hopfield, J.J., Leibler, S., and Murray, A.W. (1999). From molecular to modular cell biology. Nature *402*, C47–C52.

Jeffery, C.J. (1999). Moonlighting proteins. Trends Biochem. Sci. *24*, 8–11.

Li, S.C., Squires, C.L., and Squires, C. (1984). Antitermination of *E. coli* rRNA transcription is caused by a control region segment containing lambda nut-like sequences. Cell *38*, 851–860.

Lindahl, L., and Zengel, J.M. (1986). Ribosomal genes in Escherichia coli. Annu. Rev. Genet. *20*, 297–326.

Lindahl, L., Archer, R., and Zengel, J.M. (1983). Transcription of the S10 ribosomal protein operon is regulated by an attenuator in the leader. Cell *33*, 241–248.

Lingel, A., Simon, B., Izaurralde, E., and Sattler, M. (2003). Structure and nucleic-acid binding of the Drosophila Argonaute 2 PAZ domain. Nature *426*, 465–469.

Liu, S., Li, P., Dybkov, O., Nottrott, S., Hartmuth, K., Lührmann, R., Carlomagno, T., and Wahl, M.C. (2007). Binding of the human Prp31 Nop domain to a composite RNA-protein platform in U4 snRNP. Science *316*, 115–120.

Lüttgen, H., Robelek, R., Muhlberger, R., Diercks, T., Schuster, S.C., Kohler, P., Kessler, H., Bacher, A., and Richter, G. (2002). Transcriptional regulation by antitermination. Interaction of RNA with NusB protein and NusB/NusE protein complex of Escherichia coli. J. Mol. Biol. *316*, 875–885.

Mah, T.F., Kuznedelov, K., Mushegian, A., Severinov, K., and Greenblatt, J. (2000). The alpha subunit of E. coli RNA polymerase activates RNA binding by NusA. Genes Dev. *14*, 2664–2675.

Mason, S.W., and Greenblatt, J. (1991). Assembly of transcription elongation complexes containing the N protein of phage lambda and the Escherichia coli elongation factors NusA, NusB, NusG, and S10. Genes Dev. *5*, 1504–1512.

Mason, S.W., Li, J., and Greenblatt, J. (1992). Direct interaction between two Escherichia coli transcription antitermination factors, NusB and ribosomal protein S10. J. Mol. Biol. *223*, 55–66.

Mizushima, S., and Nomura, M. (1970). Assembly mapping of 30S ribosomal proteins from E. coli. Nature *226*, 1214.

Mogridge, J., Mah, T.F., and Greenblatt, J. (1995). A protein-RNA interaction network facilitates the template-independent cooperative assembly on RNA polymerase of a stable antitermination complex containing the lambda N protein. Genes Dev. *9*, 2831–2845.

Mogridge, J., Mah, T.F., and Greenblatt, J. (1998). Involvement of boxA nucleotides in the formation of a stable ribonucleoprotein complex containing the bacteriophage lambda N protein. J. Biol. Chem. *273*, 4143–4148.

Nodwell, J.R., and Greenblatt, J. (1991). The nut site of bacteriophage lambda is made of RNA and is bound by transcription antitermination factors on the surface of RNA polymerase. Genes Dev. *5*, 2141–2151.

Nodwell, J.R., and Greenblatt, J. (1993). Recognition of boxA antiterminator RNA by the *E. coli* antitermination factors NusB and ribosomal protein S10. Cell *72*, 261–268.

Phadtare, S., Kazakov, T., Bubunenko, M., Court, D.L., Pestova, T., and Severinov, K. (2007). Transcription antitermination by translation initiation factor IF1. J. Bacteriol. *189*, 4087–4093.

Quan, S., Zhang, N., French, S., and Squires, C.L. (2005). Transcriptional polarity in rRNA operons of Escherichia coli nusA and nusB mutant strains. J. Bacteriol. *187*, 1632–1638.

Robert, J., Sloan, S.B., Weisberg, R.A., Gottesman, M.E., Robledo, R., and Harbrecht, D. (1987). The remarkable specificity of a new transcription termination factor suggests that the mechanisms of termination and antitermination are similar. Cell *51*, 483–492.

Robledo, R., Atkinson, B.L., and Gottesman, M.E. (1991). Escherichia coli mutations that block transcription termination by phage HK022 Nun protein. J. Mol. Biol. *220*, 613–619.

Schluenzen, F., Tocilj, A., Zarivach, R., Harms, J., Gluehmann, M., Janell, D., Bashan, A., Bartels, H., Agmon, I., Franceschi, F., and Yonath, A. (2000). Structure of functionally activated small ribosomal subunit at 3.3 angstroms resolution. Cell *102*, 615–623.

Schuwirth, B.S., Borovinskaya, M.A., Hau, C.W., Zhang, W., Vila-Sanjurjo, A., Holton, J.M., and Cate, J.H. (2005). Structures of the bacterial ribosome at 3.5 Å resolution. Science *310*, 827–834.

Selmer, M., Dunham, C.M., Murphy, F.V., 4th, Weixlbaumer, A., Petry, S., Kelley, A.C., Weir, J.R., and Ramakrishnan, V. (2006). Structure of the 70S ribosome complexed with mRNA and tRNA. Science *313*, 1935–1942.

Squires, C.L., and Zaporojets, D. (2000). Proteins shared by the transcription and translation machines. Annu. Rev. Microbiol. *54*, 775–798.

Torres, M., Condon, C., Balada, J.M., Squires, C., and Squires, C.L. (2001). Ribosomal protein S4 is a transcription factor with properties remarkably similar to NusA, a protein involved in both non-ribosomal and ribosomal RNA antitermination. EMBO J. *20*, 3811–3820.

Ward, D.F., DeLong, A., and Gottesman, M.E. (1983). Escherichia coli nusB mutations that suppress nusA1 exhibit lambda N specificity. J. Mol. Biol. *168*, 73–85.

Weisberg, R.A., and Gottesman, M.E. (1999). Processive antitermination. J. Bacteriol. *181*, 359–367.

Whalen, W.A., and Das, A. (1990). Action of an RNA site at a distance: role of the nut genetic signal in transcription antitermination by phage-lambda N gene product. New Biol. *2*, 975–991.

Wimberly, B.T., Brodersen, D.E., Clemons, W.M., Morgan-Warren, R.J., Carter, A.P., Vonrhein, C., Hartsch, T., and Ramakrishnan, V. (2000). Structure of the 30S ribosomal subunit. Nature *407*, 327–339.

Wool, I.G. (1996). Extraribosomal functions of ribosomal proteins. Trends Biochem. Sci. *21*, 164–165.

Worbs, M., Huber, R., and Wahl, M.C. (2000). Crystal structure of ribosomal protein L4 shows RNA-binding sites for ribosome incorporation and feedback control of the S10 operon. EMBO J. *19*, 807–818.

Worbs, M., Bourenkov, G.P., Bartunik, H.D., Huber, R., and Wahl, M.C. (2001). An extended RNA binding surface through arrayed S1 and KH domains in transcription factor NusA. Mol. Cell *7*, 1177–1189.

Zellars, M., and Squires, C.L. (1999). Antiterminator-dependent modulation of transcription elongation rates by NusB and NusG. Mol. Microbiol. *32*, 1296–1304.

Zengel, J.M., Jerauld, A., Walker, A., Wahl, M.C., and Lindahl, L. (2003). The extended loops of ribosomal proteins L4 and L22 are not required for ribosome assembly or L4-mediated autogenous control. RNA *9*, 1188–1197.